

## Research Article

# Thrust Vector Control of an Upper-Stage Rocket with Multiple Propellant Slosh Modes

**Jaime Rubio Hervas and Mahmut Reyhanoglu**

*Department of Physical Sciences, Embry-Riddle Aeronautical University, Daytona Beach, FL 32114, USA*

Correspondence should be addressed to Mahmut Reyhanoglu, [reyhanom@erau.edu](mailto:reyhanom@erau.edu)

Received 24 May 2012; Revised 4 July 2012; Accepted 4 July 2012

Academic Editor: J. Rodellar

Copyright © 2012 J. Rubio Hervas and M. Reyhanoglu. This is an open access article distributed under the Creative Commons Attribution License, which permits unrestricted use, distribution, and reproduction in any medium, provided the original work is properly cited.

The thrust vector control problem for an upper-stage rocket with propellant slosh dynamics is considered. The control inputs are defined by the gimbal deflection angle of a main engine and a pitching moment about the center of mass of the spacecraft. The rocket acceleration due to the main engine thrust is assumed to be large enough so that surface tension forces do not significantly affect the propellant motion during main engine burns. A multi-mass-spring model of the sloshing fuel is introduced to represent the prominent sloshing modes. A nonlinear feedback controller is designed to control the translational velocity vector and the attitude of the spacecraft, while suppressing the sloshing modes. The effectiveness of the controller is illustrated through a simulation example.

## 1. Introduction

In fluid mechanics, liquid slosh refers to the movement of liquid inside an accelerating tank or container. Important examples include propellant slosh in spacecraft tanks and rockets (especially upper stages), cargo slosh in ships and trucks transporting liquids, and liquid slosh in robotically controlled moving containers.

A variety of passive methods have been employed to mitigate the adverse effect of sloshing, such as introducing baffles or partitions inside the tanks [1, 2]. These techniques do not completely succeed in canceling the sloshing effects. Thus, active control methods have been proposed for the suppression of sloshing effectively.

The control approaches developed for robotic systems moving liquid filled containers [3–11] and for accelerating space vehicles are mostly based on linear control design methods [12, 13] and adaptive control methods [14]. The linear control laws for the suppression of the slosh dynamics inevitably lead to excitation of the transverse vehicle motion through coupling effects. The complete nonlinear dynamics formulation in this paper allows simultaneous control of the transverse, pitch, and slosh dynamics.

Some of the control design methods use command input shaping methods that do not require sensor measurements of the sloshing liquid [3, 8–11], while others require either sensor measurements [4, 5] or observer estimates of the slosh states [15]. In most of these approaches, only the first sloshing mode represented by a single pendulum model or a single mass-spring model has been considered and higher slosh modes have been ignored. The literature that considers more than one sloshing mode in modeling the slosh dynamics includes [2, 16].

In this paper, a mechanical-analogy model is developed to characterize the propellant sloshing during a typical thrust vector control maneuver. The spacecraft acceleration due to the main engine thrust is assumed to be large enough so that surface tension forces do not significantly affect the propellant motion during main engine burns. This situation corresponds to a “high- $g$ ” (here  $g$  refers to spacecraft acceleration) regime that can be characterized by using the Bond number  $Bo$ —the ratio of acceleration-related forces to the liquid propellants surface tension forces, which is given by

$$Bo = \frac{\rho a R^2}{\sigma}, \quad (1.1)$$

where  $\rho$  and  $\sigma$  denote the liquid propellants density and surface tension, respectively,  $a$  is the spacecraft acceleration, and  $R$  is a characteristic dimension (e.g., propellant tank radius). During the steady-state high- $g$  situation, the propellant settles at the “bottom” of the tank with a flat free surface. When the main engine operation for thrust vector control introduces lateral accelerations, the propellant begins sloshing. As discussed in [17], Bond numbers as low as 100 would indicate that low-gravity effects may be of some significance. A detailed discussion of low-gravity fluid mechanics is given in [2].

The previous work in [16] considered a spacecraft with multiple fuel slosh modes assuming constant physical parameters. In this paper, these results are extended to account for the time-varying nature of the slosh parameters, which renders stability analysis more difficult. The control inputs are defined by the gimbal deflection angle of a nonthrottled thrust engine and a pitching moment about the center of mass of the spacecraft. The control objective, as is typical in a thrust vector control design for a liquid upper stage spacecraft during orbital maneuvers, is to control the translational velocity vector and the attitude of the spacecraft, while attenuating the sloshing modes characterizing the internal dynamics. The results are applied to the AVUM upper stage—the fourth stage of the European launcher Vega [18]. The main contributions in this paper are (i) the development of a full nonlinear mathematical model with time-varying slosh parameters and (ii) the design of a nonlinear time-varying feedback controller. A simulation example is included to illustrate the effectiveness of the controller.

## 2. Mathematical Model

This section formulates the dynamics of a spacecraft with a single propellant tank including the prominent fuel slosh modes. The spacecraft is represented as a rigid body (base body) and the sloshing fuel masses as internal bodies. In this paper, a Newtonian formulation is employed to express the equations of motion in terms of the spacecraft translational velocity

vector, the angular velocity, and the internal (shape) coordinates representing the slosh modes. A multi-mass-spring model is derived for the sloshing fuel, where the oscillation frequencies of the mass-spring elements represent the prominent sloshing modes [19].

Consider a rigid spacecraft moving on a plane as indicated in Figure 1, where  $v_x, v_z$  are the axial and transverse components, respectively, of the velocity of the center of the fuel tank, and  $\theta$  denotes the attitude angle of the spacecraft with respect to a fixed reference. The fluid is modeled by moment of inertia  $I_0$  assigned to a rigidly attached mass  $m_0$  and point masses  $m_i, i = 1, \dots, N$ , whose relative positions along the spacecraft fixed  $z$ -axis are denoted by  $s_i$ . Moments of inertia  $I_i$  of these masses are usually negligible. The locations  $h_0$  and  $h_i$  are referenced to the center of the tank. A restoring force  $-k_i s_i$  acts on the mass  $m_i$  whenever the mass is displaced from its neutral position  $s_i = 0$ . A thrust  $F$  is produced by a gimballed thrust engine as shown in Figure 1, where  $\delta$  denotes the gimbal deflection angle, which is considered as one of the control inputs. A pitching moment  $M$  is also available for control purposes. The constants in the problem are the spacecraft mass  $m$  and moment of inertia  $I$ , the distance  $b$  between the body  $z$ -axis and the spacecraft center of mass location along the longitudinal axis, and the distance  $d$  from the gimbal pivot to the spacecraft center of mass. If the tank center is in front of the spacecraft center of mass, then  $b > 0$ . The parameters  $m_0, m_i, h_0, h_i, k_i$ , and  $I_0$  depend on the shape of the fuel tank, the characteristics of the fuel and the fill ratio of the fuel tank. Note that these parameters are time-varying, which renders the Lyapunov-based stability analysis more difficult.

To preserve the static properties of the liquid, the sum of all the masses must be the same as the fuel mass  $m_f$ , and the center of mass of the model must be at the same elevation as that of the fuel, that is,

$$\begin{aligned} m_0 + \sum_{i=1}^N m_i &= m_f, \\ m_0 h_0 + \sum_{i=1}^N m_i h_i &= 0. \end{aligned} \quad (2.1)$$

Assuming a constant fuel burn rate, we have

$$m_f = m_{\text{ini}} \left( 1 - \frac{t}{t_f} \right), \quad (2.2)$$

where  $m_{\text{ini}}$  is the initial fuel mass in the tank and  $t_f$  is the time at which, at a constant rate, all the fuel is burned.

To compute the slosh parameters, a simple equivalent cylindrical tank is considered together with the model described in [2], which can be summarized as follows. Assuming a constant propellant density, the height of still liquid inside the cylindrical tank is

$$h = \frac{4m_f}{\pi \varphi^2 \rho}, \quad (2.3)$$



Let  $\hat{i}$  and  $\hat{k}$  be the unit vectors along the spacecraft-fixed longitudinal and transverse axes, respectively, and denote by  $(x, z)$  the inertial position of the center of the fuel tank. The position vector of the center of mass of the vehicle can then be expressed in the spacecraft-fixed coordinate frame as

$$\vec{r} = (x - b)\hat{i} + z\hat{k}. \quad (2.9)$$

The inertial velocity and acceleration of the vehicle can be computed as

$$\begin{aligned} \dot{\vec{r}} &= v_x\hat{i} + (v_z + b\dot{\theta})\hat{k}, \\ \ddot{\vec{r}} &= (a_x + b\dot{\theta}^2)\hat{i} + (a_z + b\ddot{\theta})\hat{k}, \end{aligned} \quad (2.10)$$

where we have used the fact that  $(v_x, v_z) = (\dot{x} + z\dot{\theta}, \dot{z} - x\dot{\theta})$  and  $(a_x, a_z) = (\dot{v}_x + v_z\dot{\theta}, \dot{v}_z - v_x\dot{\theta})$ .

Similarly, the position vectors of the fuel masses  $m_0, m_i$ , for all  $i$ , in the spacecraft-fixed coordinate frame are given, respectively, by

$$\begin{aligned} \vec{r}_0 &= (x + h_0)\hat{i} + z\hat{k}, \\ \vec{r}_i &= (x + h_i)\hat{i} + (z + s_i)\hat{k}, \quad \forall i. \end{aligned} \quad (2.11)$$

The inertial accelerations of the fuel masses can be computed as

$$\begin{aligned} \ddot{\vec{r}}_0 &= (a_x - h_0\dot{\theta}^2 + \ddot{h}_0)\hat{i} + (a_z - 2h_0\dot{\theta} - h_0\ddot{\theta})\hat{k}, \\ \ddot{\vec{r}}_i &= (a_x + s_i\ddot{\theta} - h_i\dot{\theta}^2 + \ddot{h}_i + 2s_i\dot{\theta})\hat{i} + (a_z + s_i\ddot{\theta} - h_i\dot{\theta} - s_i\dot{\theta}^2 - 2h_i\dot{\theta})\hat{k}, \quad \forall i. \end{aligned} \quad (2.12)$$

Now Newton's second law for the whole system can be written as

$$\vec{F} = m\ddot{\vec{r}} + \sum_{i=0}^N m_i\ddot{\vec{r}}_i, \quad (2.13)$$

where

$$\vec{F} = F(\hat{i} \cos \delta + \hat{k} \sin \delta). \quad (2.14)$$

The total torque with respect to the tank center can be expressed as

$$\vec{\tau} = \left( I + I_0 + \sum_{i=1}^N I_i \right) \ddot{\theta} \hat{j} + \vec{\rho} \times m\ddot{\vec{r}} + \sum_{i=0}^N \vec{\rho}_i \times m\ddot{\vec{r}}_i, \quad (2.15)$$

where

$$\vec{\tau} = \tau \hat{j} = [M + F(b + d) \sin \delta] \hat{j}, \quad (2.16)$$

and  $\vec{\rho}, \vec{\rho}_0$ , and  $\vec{\rho}_i$  are the positions of  $m, m_0$ , and  $m_i$  relative to the tank center, respectively, that is,

$$\vec{\rho} = -b\hat{i}, \quad \vec{\rho}_0 = h_0\hat{i}, \quad \vec{\rho}_i = h_i\hat{i} + s_i\hat{k}, \quad \forall i. \quad (2.17)$$

The dissipative effects due to fuel slosh are included via damping constants  $c_i$ . When the damping is small, it can be represented accurately by equivalent linear viscous damping. Newton's second law for the fuel mass  $m_i$  can be written as

$$m_i a_{z_i} = -c_i \dot{s}_i - k_i s_i, \quad (2.18)$$

where

$$a_{z_i} = \ddot{s}_i + a_z - h_i \ddot{\theta} - s_i \dot{\theta}^2 - 2\dot{h}_i \dot{\theta}. \quad (2.19)$$

Using (2.13)–(2.18), the equations of motion can be obtained as

$$(m + m_f) a_x + mb\dot{\theta}^2 + \sum_{i=1}^N m_i (s_i \ddot{\theta} + 2\dot{s}_i \dot{\theta} + \ddot{h}_i) + m_0 \ddot{h}_0 = F \cos \delta, \quad (2.20)$$

$$(m + m_f) a_z + mb\ddot{\theta} + \sum_{i=1}^N m_i (\ddot{s}_i - s_i \dot{\theta}^2 - 2\dot{h}_i \dot{\theta}) - 2m_0 \dot{h}_0 \dot{\theta} = F \sin \delta, \quad (2.21)$$

$$\hat{I} \ddot{\theta} + \sum_{i=1}^N m_i (s_i a_x - h_i \ddot{s}_i + 2(s_i \dot{s}_i + h_i \dot{h}_i) \dot{\theta} + s_i \ddot{h}_i) + 2m_0 h_0 \dot{h}_0 \dot{\theta} + mba_z = \tau, \quad (2.22)$$

$$m_i (\ddot{s}_i + a_z - h_i \ddot{\theta} - s_i \dot{\theta}^2 - 2\dot{h}_i \dot{\theta}) + k_i s_i + c_i \dot{s}_i = 0, \quad \forall i, \quad (2.23)$$

where  $p = b + d$  and

$$\hat{I} = I + I_0 + mb^2 + m_0 h_0^2 + \sum_{i=1}^N [I_i + m_i (h_i^2 + s_i^2)]. \quad (2.24)$$

The control objective is to design feedback controllers so that the controlled spacecraft accomplishes a given planar maneuver, that is a change in the translational velocity vector and the attitude of the spacecraft, while suppressing the fuel slosh modes. Equations (2.20)–(2.23) model interesting examples of underactuated mechanical systems. The published literature on the dynamics and control of such systems includes the development of theoretical controllability and stabilizability results for a large class of systems using tools from nonlinear control theory and the development of effective nonlinear control design methodologies [20] that are applied to several practical examples, including underactuated space vehicles [21, 22] and underactuated manipulators [23].

### 3. Nonlinear Feedback Controller

This section presents a detailed development of feedback control laws through the model obtained via the multi-mass-spring analogy.

Consider the model of a spacecraft with a gimballed thrust engine shown in Figure 1. If the thrust  $F$  during the fuel burn is a positive constant, and if the gimbal deflection angle and pitching moment are zero,  $\delta = M = 0$ , then the spacecraft and fuel slosh dynamics have a relative equilibrium defined by

$$v_z = \bar{v}_z, \quad \theta = \bar{\theta}, \quad \dot{\theta} = 0, \quad s_i = 0, \quad \dot{s}_i = 0, \quad \forall i, \quad (3.1)$$

where  $\bar{v}_z$  and  $\bar{\theta}$  are arbitrary constants. Without loss of generality, the subsequent analysis considers the relative equilibrium at the origin, that is,  $\bar{v}_z = \bar{\theta} = 0$ . Note that the relative equilibrium corresponds to the vehicle axial velocity

$$v_x(t) = v_{x_0} + \bar{a}_x t, \quad t \leq t_b, \quad (3.2)$$

where  $v_{x_0}$  is the initial axial velocity of the spacecraft,  $t_b$  is the fuel burn time, and

$$\bar{a}_x = \frac{F}{m + m_f}. \quad (3.3)$$

Now assume the axial acceleration term  $a_x$  is not significantly affected by small gimbal deflections, pitch changes, and fuel motion (an assumption verified in simulations). Consequently, (2.20) becomes

$$\dot{v}_x + \dot{\theta} v_z = \bar{a}_x. \quad (3.4)$$

Substituting this approximation leads to the following reduced equations of motion for the transverse, pitch, and slosh dynamics:

$$(m + m_f) \hat{a}_z + mb\ddot{\theta} + \sum_{i=1}^N m_i (\ddot{s}_i - s_i \dot{\theta}^2 - 2\dot{h}_i \dot{\theta}) - 2m_0 \dot{h}_0 \dot{\theta} = F \sin \delta, \quad (3.5)$$

$$\hat{I} \ddot{\theta} + \sum_{i=1}^N m_i [\bar{a}_x s_i - h_i \ddot{s}_i + s_i \ddot{h}_i + 2(s_i \dot{s}_i + h_i \dot{h}_i) \dot{\theta}] + 2m_0 h_0 \dot{h}_0 \dot{\theta} + mb \hat{a}_z = \tau, \quad (3.6)$$

$$m_i (\ddot{s}_i + \hat{a}_z - h_i \ddot{\theta} - s_i \dot{\theta}^2 - 2\dot{h}_i \dot{\theta}) + k_i s_i + c_i \dot{s}_i = 0, \quad \forall i, \quad (3.7)$$

where  $\hat{a}_z = \dot{v}_z - \dot{\theta} v_x(t)$ . Here  $v_x(t)$  is considered as an exogenous input. The subsequent analysis is based on the above equations of motion for the transverse, pitch, and slosh dynamics of the vehicle.

Eliminating  $\ddot{s}_i$  in (3.5) and (3.6) using (3.7) yields

$$\begin{aligned} (m + m_0)\hat{a}_z + (mb - m_0h_0)\ddot{\theta} - 2m_0\dot{h}_0\dot{\theta} - \sum_{i=1}^N (k_i s_i + c_i \dot{s}_i) &= F \sin \delta, \\ (mb - m_0h_0)\hat{a}_z + \left( \hat{I} - \sum_{i=1}^N m_i h_i^2 \right) \ddot{\theta} + 2m_0 h_0 \dot{h}_0 \dot{\theta} + G &= M + Fp \sin \delta, \end{aligned} \quad (3.8)$$

where

$$G = \sum_{i=1}^N \left[ (m_i \bar{a}_x + m_i \ddot{h}_i + k_i h_i) s_i + h_i c_i \dot{s}_i + 2m_i s_i \dot{s}_i \dot{\theta} - m_i h_i s_i \dot{\theta}^2 \right]. \quad (3.9)$$

Note that the expressions (2.1) have been utilized to obtain (3.8) in the form above.

By defining control transformations from  $(\delta, M)$  to new control inputs  $(u_1, u_2)$ :

$$\begin{bmatrix} u_1 \\ u_2 \end{bmatrix} = \begin{bmatrix} m + m_0 & mb - m_0 h_0 \\ mb - m_0 h_0 & \hat{I} - \sum_{i=1}^N m_i h_i^2 \end{bmatrix}^{-1} \begin{bmatrix} F \sin \delta + 2m_0 \dot{h}_0 \dot{\theta} + \sum_{i=1}^N (k_i s_i + c_i \dot{s}_i) \\ M + Fp \sin \delta - 2m_0 h_0 \dot{h}_0 \dot{\theta} - G \end{bmatrix}, \quad (3.10)$$

the system (3.5)–(3.7) can be written as

$$\dot{v}_z = u_1 + \dot{\theta} v_x(t), \quad (3.11)$$

$$\ddot{\theta} = u_2, \quad (3.12)$$

$$\ddot{s}_i = -\omega_i^2 s_i - 2\zeta_i \omega_i \dot{s}_i - u_1 + h_i u_2 + s_i \dot{\theta}^2 + 2\dot{h}_i \dot{\theta}, \quad \forall i, \quad (3.13)$$

where

$$\omega_i^2 = \frac{k_i}{m_i}, \quad 2\zeta_i \omega_i = \frac{c_i}{m_i}, \quad \forall i. \quad (3.14)$$

Here  $\omega_i$  and  $\zeta_i$ , for all  $i$ , denote the undamped natural frequencies and damping ratios, respectively.

The main idea in the subsequent development is to first design feedback control laws for  $(u_1, u_2)$  and then use the following equations to obtain the feedback laws for the original controls  $(\delta, M)$  for  $t \leq t_b$ :

$$\delta = \sin^{-1} \left( \frac{\left[ (m + m_0)u_1 + (mb - m_0h_0)u_2 - 2m_0\dot{h}_0\dot{\theta} - \sum_{i=1}^N (k_i s_i + c_i \dot{s}_i) \right]}{F} \right), \quad (3.15)$$

$$M = (mb - m_0h_0)u_1 + \left( \hat{I} - \sum_{i=1}^N m_i h_i^2 \right) u_2 + 2m_0 h_0 \dot{h}_0 \dot{\theta} + G - Fp \sin \delta. \quad (3.16)$$



Consider the following candidate Lyapunov function to stabilize the subsystem defined by (3.11) and (3.12):

$$V = \frac{r_1}{2}v_z^2 + \frac{r_2}{2}\theta^2 + \frac{r_3}{2}\dot{\theta}^2, \quad (3.17)$$

where  $r_1, r_2$ , and  $r_3$  are positive constants so that the function  $V$  is positive definite.

The time derivative of  $V$  along the trajectories of (3.11) and (3.12) can be computed as

$$\dot{V} = r_1v_z\dot{v}_z + r_2\theta\dot{\theta} + r_3\dot{\theta}\ddot{\theta} \quad (3.18)$$

or rewritten in terms of the new control inputs

$$\dot{V} = (r_1v_z)u_1 + (r_1v_xv_z + r_2\theta + r_3u_2)\dot{\theta}. \quad (3.19)$$

Clearly, the feedback laws

$$u_1 = -l_1v_z, \quad (3.20)$$

$$u_2 = -\frac{1}{r_3}(r_2\theta + l_2\dot{\theta}), \quad (3.21)$$

where  $l_1, l_2$  are positive constants and taking into account that

$$r_1v_xv_z\dot{\theta} \leq \left( \frac{\dot{\theta}^2}{2} + \frac{(r_1v_xv_z)^2}{2} \right), \quad (3.22)$$

yield

$$\begin{aligned} \dot{V} &= -l_1r_1v_z^2 - l_2\dot{\theta}^2 + r_1v_xv_z\dot{\theta} \\ &\leq -r_1\left(l_1 - \frac{r_1v_x^2}{2}\right)v_z^2 - \left(l_2 - \frac{1}{2}\right)\dot{\theta}^2, \end{aligned} \quad (3.23)$$

which satisfies  $\dot{V} \leq 0$  if  $l_1 > 0.5r_1v_x^2$  and  $l_2 > 0.5$ .

The closed-loop system for  $(v_z, \theta)$ -dynamics can be written as

$$\dot{v}_z = -l_1v_z + \dot{\theta}v_x(t), \quad (3.24)$$

$$\ddot{\theta} = -K_1\theta - K_2\dot{\theta}, \quad (3.25)$$

where  $K_1 = r_2/r_3$  and  $K_2 = l_2/r_3$ .

Equation (3.25) can be easily solved in the case of  $K_2^2 > 4K_1$  as

$$\theta(t) = Ae^{-\lambda_1 t} + Be^{-\lambda_2 t}, \quad (3.26)$$

where  $A, B$  are integration constants and  $-\lambda_1, -\lambda_2$  are the eigenvalues of the linear system (3.25). Therefore,  $\theta(t)$  and  $\dot{\theta}(t)$  can be upper bounded as

$$|\theta(t)| \leq Ce^{-\lambda t}, \quad |\dot{\theta}(t)| \leq De^{-\lambda t}, \quad (3.27)$$

respectively, where  $C, D$  are positive constants and  $\lambda = \min(\lambda_1, \lambda_2)$ . Now, assuming that  $\lambda \neq l_1$ , (3.24) can be integrated to obtain an upper bound for  $v_z(t)$  as

$$|v_z(t)| \leq \alpha e^{-\beta t}, \quad (3.28)$$

where  $\alpha, \beta$  are positive constants. Therefore, it can be concluded that the  $(v_z, \theta)$ -dynamics are exponentially stable under the control laws (3.20) and (3.21).

To analyze the stability of the  $N$  equations defined by (3.13), it will be first shown that the system described by the equation

$$\ddot{s}_i + 2\zeta_i \omega_i(t) \dot{s}_i + \omega_i^2(t) s_i = 0 \quad (3.29)$$

is exponentially stable.

From (2.4) and (2.6),

$$\omega_i(t) = \sqrt{\frac{2g\xi_i}{\varphi} \tanh\left(\frac{2\xi_i h(t)}{\varphi}\right)} \in C^1. \quad (3.30)$$

The following properties can be shown to hold:

$$\begin{aligned} \omega_i^2(t) &\geq \varepsilon_1^2, & p(t) &= \frac{1}{2} \frac{\dot{\omega}_i(t)}{\omega_i(t)} + 2\zeta_i \omega_i(t) \geq \varepsilon_2^2, \\ |2\zeta_i \omega_i(t)| &\leq 2\zeta_i \sqrt{\frac{2g\xi_i}{\varphi}} = M_1, & |\omega_i^2(t)| &\leq \frac{2g\xi_i}{\varphi} = M_2, \\ |2\dot{\omega}_i(t)\omega_i(t)| &\leq g \left(\frac{2\xi_i}{\varphi}\right)^2 = M_3, \end{aligned} \quad (3.31)$$

where  $\varepsilon_1$  and  $\varepsilon_2$  are small positive parameters given the fact that the tank will never be totally empty, but a small amount of fuel will always remain inside. For this same reason,  $h(t) > 0$ , for all  $t$ . Therefore, by Corollary A.2 in the Appendix, the system (3.29) is exponentially stable.

Now write (3.13) as

$$\dot{x} = (A_1(t) + A_2(t))x + H(t), \quad (3.32)$$

**Table 1:** Physical parameters for AVUM stage of Vega.

Parameter	Value	Parameter	Value
$T$	2.45 kN	$b$	-0.6 m
$m$	975 kg	$d$	1.2 m
$m_{\text{ini}}$	580 kg	$\varphi$	1 m
$I$	400 kg·m <sup>2</sup>	$t_b$	650 s
$I_1$	10 kg·m <sup>2</sup>	$t_f$	667 s
$I_2$	1 kg·m <sup>2</sup>	$\rho$	1180 kg/m <sup>3</sup>

where  $x = [s_i, \dot{s}_i]^T$  and

$$\begin{aligned}
 A_1(t) &= \begin{bmatrix} 0 & 1 \\ -\omega_i^2(t) & -2\zeta_i\omega_i(t) \end{bmatrix}, & A_2(t) &= \begin{bmatrix} 0 & 0 \\ \dot{\theta}^2(t) & 0 \end{bmatrix}, \\
 H(t) &= \begin{bmatrix} 0 \\ -\hat{a}_z(t) + h_i(t)\ddot{\theta}(t) + 2\dot{h}_i(t)\dot{\theta}(t) \end{bmatrix}.
 \end{aligned} \tag{3.33}$$

Under the stated assumptions,  $A_1(t)$  is exponentially stable (see the Appendix) and there exist positive constants  $\lambda_0$ ,  $\lambda_1$ , and  $\lambda_2$  such that

$$\int_0^\infty \|A_2(t)\| dt \leq \lambda_0, \quad \|H(t)\| \leq \lambda_1 e^{-\lambda_2 t}, \quad \forall t \geq 0. \tag{3.34}$$

Hence, for any initial condition, the state of the system (3.5)–(3.7) converges exponentially to zero.

## 4. Simulation

The feedback control law developed in the previous section is implemented here for the fourth stage of the European launcher Vega. The first two slosh modes are included to demonstrate the effectiveness of the controller (3.15), (3.16), (3.20), (3.21) by applying to the complete nonlinear system (2.20)–(2.23). The physical parameters used in the simulations are given in Table 1.

We consider stabilization of the spacecraft in orbital transfer, suppressing the transverse and pitching motion of the spacecraft and sloshing of fuel while the spacecraft is accelerating. In other words, the control objective is to stabilize the relative equilibrium corresponding to a specific spacecraft axial acceleration and  $v_z = \theta = \dot{\theta} = s_i = \dot{s}_i = 0$ ,  $i = 1, 2$ .

Time responses shown in Figures 2, 3, and 4 correspond to the initial conditions  $v_{x_0} = 3000$  m/s,  $v_{z_0} = 100$  m/s,  $\theta_0 = 5^\circ$ ,  $\dot{\theta}_0 = 0$ ,  $s_{1_0} = 0.1$  m,  $s_{2_0} = -0.1$  m, and  $\dot{s}_{1_0} = \dot{s}_{2_0} = 0$ . We assume a fuel burn time of 650 seconds. As can be seen, the transverse velocity, attitude angle, and the slosh states converge to the relative equilibrium at zero while the axial velocity  $v_x$  increases and  $\dot{v}_x$  tends asymptotically to  $F/(m + m_f)$ . Note that there is a trade-off between good responses for the directly actuated degrees of freedom (the transverse and pitch dynamics) and good responses for the internal degrees of freedom (the slosh dynamics); the controller given by (3.15), (3.16), (3.20), (3.21) with parameters  $r_1 = 8 \times 10^{-7}$ ,  $r_2 = 10^3$ ,  $r_3 = 500$ ,  $l_1 = 10^4$ , and  $l_2 = 4 \times 10^4$  represents one example of this balance.

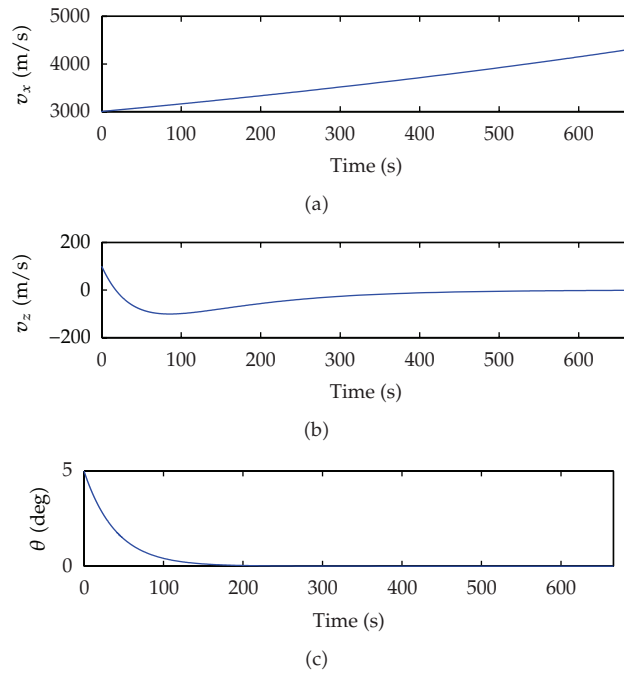


**Figure 2:** Time responses of  $v_x$ ,  $v_z$ , and  $\theta$ .

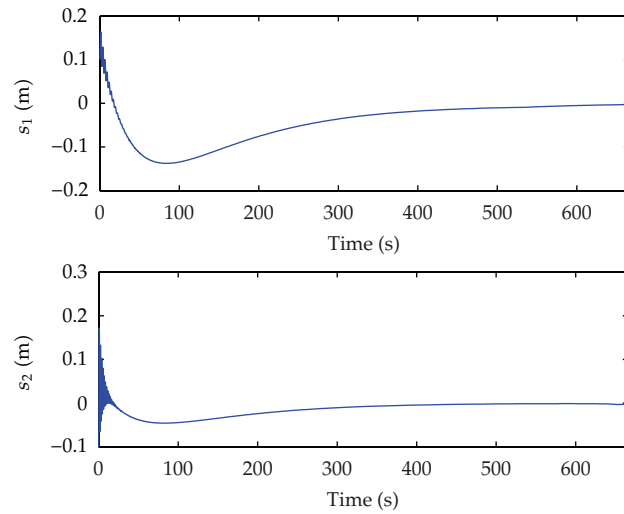


**Figure 3:** Time responses of  $s_1$  and  $s_2$ .

Figures 5, 6, and 7 show the results of a simulation with no control ( $M = \delta = 0$ ) using the same initial conditions and physical parameters as above. As expected, the fuel slosh dynamics destabilize the uncontrolled spacecraft.

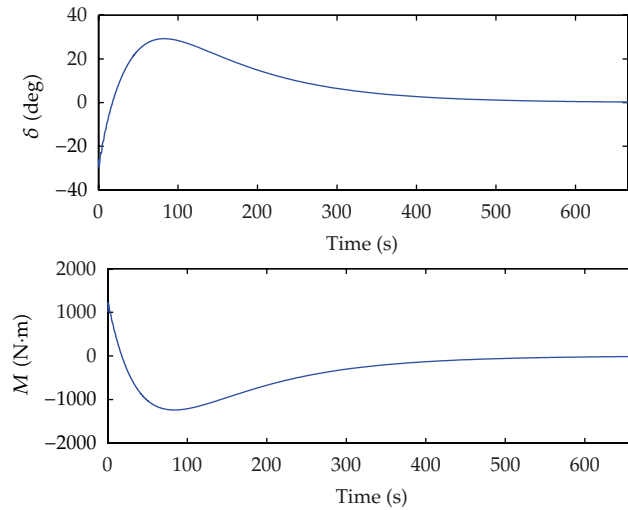


**Figure 4:** Gimbal deflection angle  $\delta$  and pitching moment  $M$ .

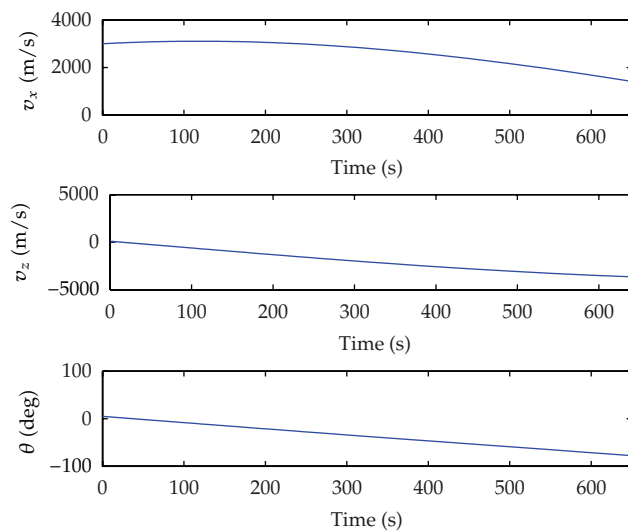


**Figure 5:** Time responses of  $v_x$ ,  $v_z$  and  $\theta$  (zero control case).

## 5. Conclusions

A complete nonlinear dynamical model has been developed for a spacecraft with multiple slosh modes that have time-varying parameters. A feedback controller has been designed to achieve stabilization of the pitch and transverse dynamics as well as suppression of the slosh modes, while the spacecraft accelerates in the axial direction. The effectiveness of the feedback controller has been illustrated through a simulation example.

The many avenues considered for future research include problems involving multiple liquid containers and three-dimensional transfers. Future research also includes designing nonlinear observers to estimate the slosh states as well as nonlinear control laws that achieve

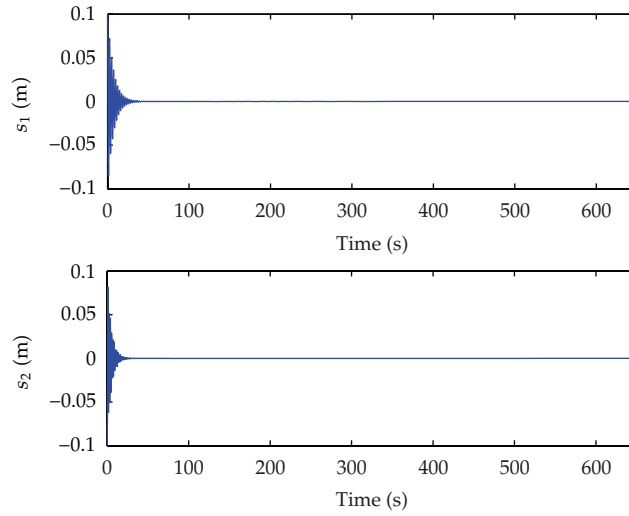


**Figure 6:** Time responses of  $s_1$  and  $s_2$  (zero control case).

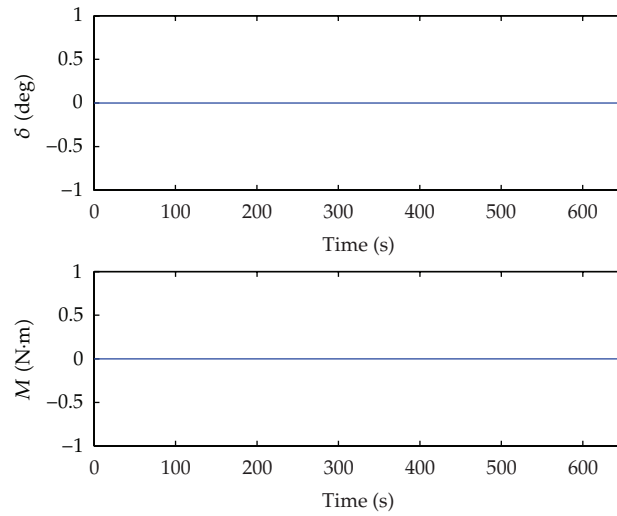


**Figure 7:** Gimbal deflection angle  $\delta$  and pitching moment  $M$  (zero control case).

robustness, insensitivity to system and control parameters, and improved disturbance rejection.

## Appendix

Consider the system

$$\ddot{s} + f(t)\dot{s} + g(t)s = 0, \quad (\text{A.1})$$

where  $g(t) \in C^1$ ,  $|f(t)| < M_1$ ,  $|g(t)| < M_2$ ,  $|\dot{g}(t)| < M_3$ .

**Theorem A.1.** *If  $g(t) > \varepsilon_1^2$  and  $p(t) = (1/2)(\dot{g}(t)/g(t)) + f(t) > \varepsilon_2^2$ , then the origin is globally uniformly asymptotically stable.*

*Proof.* Given the conditions above, the following bounds can be set:

$$\begin{aligned} -M_1 < f(t) < M_1, & \quad a_1^2 < g(t) < M_2, \\ -M_3 < \dot{g}(t) < M_3, & \quad \varepsilon_2^2 < p(t) < \frac{M_3}{2\varepsilon_1^2} + M_1. \end{aligned} \quad (\text{A.2})$$

Consider the following candidate Lyapunov function:

$$V(z, t) = \frac{1}{2} \left( s^2 + 2\beta \frac{s\dot{s}}{\sqrt{g(t)}} + \frac{\dot{s}^2}{g(t)} \right), \quad (\text{A.3})$$

where  $z = [s \ \dot{s}]^T$  is the state vector and  $\beta$  is a positive constant. This function can be rewritten in a matrix form as

$$V(z, t) = \frac{1}{2} [s \ \dot{s}] \begin{bmatrix} 1 & \frac{\beta}{\sqrt{g}} \\ \frac{\beta}{\sqrt{g}} & \frac{1}{g} \end{bmatrix} \begin{bmatrix} s \\ \dot{s} \end{bmatrix}, \quad (\text{A.4})$$

which is positive definite if  $\beta < 1$ .

Recalling that a positive definite quadratic function  $z^T P z$  satisfies

$$\lambda_{\min}(P) z^T z \leq z^T P z \leq \lambda_{\max}(P) z^T z, \quad (\text{A.5})$$

where

$$\begin{aligned} \lambda_{\min}(P) &= \frac{1+g}{2g} \left[ 1 - \sqrt{1 - 4g \frac{1-\beta^2}{(1+g)^2}} \right], \\ \lambda_{\max}(P) &= \frac{1+g}{2g} \left[ 1 + \sqrt{1 - 4g \frac{1-\beta^2}{(1+g)^2}} \right], \end{aligned} \quad (\text{A.6})$$

and thus the following hold:

$$\gamma_1 \|z\|^2 \leq V \leq \gamma_2 \|z\|^2, \quad (\text{A.7})$$

where  $\gamma_1$  and  $\gamma_2$  are positive constants.

Taking the time derivative of  $V(z, t)$  yields

$$\dot{V} = -\frac{\beta}{\sqrt{g(t)}} \left[ g(t)s^2 + p(t)s\dot{s} + \left( \frac{p(t)}{\beta\sqrt{g(t)}} - 1 \right) \dot{s}^2 \right], \quad (\text{A.8})$$

which can be rewritten as

$$\dot{V} = -\frac{\beta}{\sqrt{g}} [s \quad \dot{s}] \begin{bmatrix} g & p \\ \frac{p}{2} & \frac{p}{\beta\sqrt{g}} - 1 \end{bmatrix} \begin{bmatrix} s \\ \dot{s} \end{bmatrix} < 0. \quad (\text{A.9})$$

Clearly,  $\dot{V} < 0$  if

$$\beta < \frac{16\varepsilon_1^5\varepsilon_2^2}{16M_2\varepsilon_1^4 + (M_3 + 2\varepsilon_1^2M_1)^2}. \quad (\text{A.10})$$

Note that  $\dot{V}$  satisfies

$$\dot{V} \leq -\frac{\beta}{\sqrt{g}} \lambda_{\min}(Q) \|z\|^2. \quad (\text{A.11})$$

It can be shown that if

$$\beta < \min \left\{ 1, \frac{\varepsilon_2^2}{(1 - M_2)\sqrt{M_2}}, \frac{16\varepsilon_1^5\varepsilon_2^2}{16M_2\varepsilon_1^4 + (M_3 + 2\varepsilon_1^2M_1)^2} \right\}, \quad (\text{A.12})$$

then, using Theorem 4.10 of [24], it can be concluded that the origin is exponentially stable. Hence, the following result can be stated.  $\square$

**Corollary A.2.** *There exist  $\alpha, \beta > 0$  such that*

$$|s| < \beta e^{-\alpha(t-t_0)}, \quad |\dot{s}| < \beta e^{-\alpha(t-t_0)}, \quad \forall t \geq t_0. \quad (\text{A.13})$$

*The following result is a modified version of that presented in [20].*

**Lemma A.3.** *Consider a system that is described by the linear time-varying differential equation*

$$\dot{x} = (A_1(t) + A_2(t))x + H(t), \quad x \in \mathbb{R}^n. \quad (\text{A.14})$$

*If the matrix  $A_1(t)$  is exponentially stable and there exist positive constants  $\lambda_0, \lambda_1$ , and  $\lambda_2$  such that*

$$(i) \int_0^\infty \|A_2(t)\| dt \leq \lambda_0, \quad (ii) \|H(t)\| \leq \lambda_1 e^{-\lambda_2 t}, \quad \forall t \geq 0, \quad (\text{A.15})$$

*then all the solutions of (A.14) approach zero exponentially as  $t$  goes to  $\infty$ .*



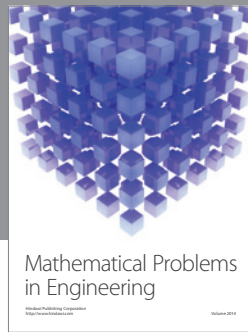
## Acknowledgment

The authors wish to acknowledge the support provided by Embry-Riddle Aeronautical University.

## References

- [1] K. C. Biswal, S. K. Bhattacharyya, and P. K. Sinha, "Dynamic characteristics of liquid filled rectangular tank with baffles," *Journal of the Institution of Engineers*, vol. 84, no. 2, pp. 145–148, 2003.
- [2] F. T. Dodge, *The New "Dynamic Behavior of Liquids in Moving Containers"*, Southwest Research Institute, San Antonio, Tex, USA, 2000.
- [3] J. T. Feddema, C. R. Dohrmann, G. G. Parker, R. D. Robinett, V. J. Romero, and D. J. Schmitt, "Control for slosh-free motion of an open container," *IEEE Control Systems Magazine*, vol. 17, no. 1, pp. 29–36, 1997.
- [4] M. Grundelius, "Iterative optimal control of liquid slosh in an industrial packaging machine," in *Proceedings of the 39th IEEE Conference on Decision and Control*, pp. 3427–3432, Dec, December 2000.
- [5] M. Grundelius and B. Bernhardsson, "Control of liquid slosh in an industrial packaging machine," in *Proceedings of the IEEE International Conference on Control Applications (CCA) and IEEE International Symposium on Computer Aided Control System Design (CACSD)*, pp. 1654–1659, August 1999.
- [6] K. Terashima and G. Schmidt, "Motion control of a cart-based container considering suppression of liquid oscillations," in *Proceedings of the 1994 IEEE International Symposium on Industrial Electronics*, pp. 275–280, May 1994.
- [7] K. Yano and K. Terashima, "Robust liquid container transfer control for complete sloshing suppression," *IEEE Transactions on Control Systems Technology*, vol. 9, no. 3, pp. 483–493, 2001.
- [8] K. Yano and K. Terashima, "Sloshing suppression control of liquid transfer systems considering a 3-D transfer path," *IEEE/ASME Transactions on Mechatronics*, vol. 10, no. 1, pp. 8–16, 2005.
- [9] A. Aboel-Hassan, M. Arafa, and A. Nassef, "Design and optimization of input shapers for liquid slosh suppression," *Journal of Sound and Vibration*, vol. 320, no. 1-2, pp. 1–15, 2009.
- [10] Q. Naiming, D. Kai, W. Xianlu, and L. Yunqian, "Spacecraft propellant sloshing suppression using input shaping technique," in *Proceedings of the International Conference on Computer Modeling and Simulation (ICCMS '09)*, pp. 162–166, Feb, February 2009.
- [11] B. Pridgen, K. Bai, and W. Singhose, "Slosh suppression by robust input shaping," in *Proceedings of the 49th IEEE Conference on Decision and Control (CDC '10)*, pp. 2316–2321, Dec, December 2010.
- [12] A. E. Bryson, *Control of Spacecraft and Aircraft*, Princeton University Press, Princeton, NJ, USA, 1994.
- [13] B. Wie, *Space Vehicle Dynamics and Control*, AIAA Education Series, Reston, Va, USA, 1998.
- [14] J. M. Adler, M. S. Lee, and J. D. Saugen, "Adaptive control of propellant slosh for launch vehicles," in *Proceedings of the Sensors and Sensor Integration*, pp. 11–22, April 1991.
- [15] B. Bandyopadhyay, P. S. Gandhi, and S. Kurode, "Sliding mode observer based sliding mode controller for slosh-free motion through PID scheme," *IEEE Transactions on Industrial Electronics*, vol. 56, no. 9, pp. 3432–3442, 2009.
- [16] M. Reyhanoglu and J. R. Hervas, "Nonlinear control of space vehicles with multi-mass fuel slosh dynamics," in *Proceedings of International Conference on Recent Advances in Space Technologies*, pp. 247–252, 2011.
- [17] P. J. Enright and E. C. Wong, "Propellant slosh models for the cassini spacecraft," in *Proceedings of AIAA/AAS Conference, AIAA-94-3730-CP*, pp. 186–195, 1994.
- [18] E. Perez, *Vega User's Manual, Issue 3*, Arianespace, Washington, DC, USA, 2006.
- [19] M. J. Sidi, *Spacecraft Dynamics and Control, Cambridge Aerospace Series*, Cambridge University Press, Cambridge, UK, 1997.
- [20] M. Reyhanoglu, S. Cho, and N. H. McClamroch, "Discontinuous feedback control of a special class of underactuated mechanical systems," *International Journal of Robust and Nonlinear Control*, vol. 10, no. 4, pp. 265–281, 2000.
- [21] H. Krishnan, H. McClamroch, and M. Reyhanoglu, "On the attitude stabilization of a rigid spacecraft using two control torques," in *Proceedings of the American Control Conference*, pp. 1990–1995, June 1992.

- [22] M. Reyhanoglu, "Maneuvering control problems for a spacecraft with unactuated fuel slosh dynamics," in *Proceedings of 2003 IEEE Conference on Control Applications*, pp. 695–699, tur, June 2003.
- [23] A. D. Mahindrakar, R. N. Banavar, and M. Reyhanoglu, "Controllability and point-to-point control of 3-DOF planar horizontal underactuated manipulators," *International Journal of Control*, vol. 78, no. 1, pp. 1–13, 2005.
- [24] H. K. Khalil, *Nonlinear Systems*, Prentice-Hall, New York, NY, USA, 3rd edition, 2002.



# Hindawi

Submit your manuscripts at  
<http://www.hindawi.com>

